https://doi.org/10.5194/egusphere-2025-1112
Preprint. Discussion started: 27 March 2025

Bias Correcting Regional Scale Earth Systems Model Projections: Novel Approach using Empirical Mode Decomposition

Arkaprabha Ganguli[1,*], Jeremy Feinstein[2,*], Ibraheem Raji[3], Akintomide Akinsanola[2,3], Connor Aghili[2], Chunyong Jung[2], Jordan Branham[4], Tom Wall[4], Whitney Huang[5], and Rao Kotamarthi[2]

[1]Mathematics and Computer Science Division, Argonne National Laboratory, Lemont, IL, USA
[2]Environmental Science Division, Argonne National Laboratory, Lemont, IL, USA
[3]Department of Earth and Environmental Sciences, University of Illinois Chicago, Chicago, IL, USA
[4]Decision and Infrastructure Sciences, Argonne National Laboratory, Lemont, IL, USA
[5]School of Mathematical and Statistical Sciences, Clemson University, Clemson, SC, USA
[*]These authors contributed equally to this work.

Correspondence: Arkaprabha Ganguli (aganguli@anl.gov) and Jeremy Feinstein (jfeinstein@anl.gov)

Abstract. Bias correction is a crucial step in using Earth systems model outputs for assessments, as it adjusts systematic errors by comparing the model to observations. However, standard methods—ranging from mean-based linear scaling to distribution-based quantile mapping typically treat bias correction as a single-scale process, overlooking the fact that biases can manifest differently across daily, seasonal, and annual timescales. In this study, we propose a novel, timescale-aware bias-correction approach built on Empirical Mode Decomposition ~~(EMD)~~. By decomposing the meteorological signal into multiple oscillatory components and aggregating them to represent distinct timescales, we apply targeted corrections to each component, thereby preserving both short- and long-term structure in the data. Experimental validations demonstrate that this finer-grained method substantially improves upon existing bias-correction techniques such as quantile mapping. As a result, the proposed approach offers a more robust path to accurate and reliable Earth systems projections, strengthening their utility for resilience and adaptation planning.

1 Introduction

Accurate projections of future weather dynamics at regional and local scales are crucial not only for understanding extremes but also for guiding decision-making in sectors such as water resource management, agriculture, renewable energy, and public health. Over the decades, the horizontal spatial resolution of large-scale models, including global climate models (GCMs), has significantly improved, with grid cells for CMIP6 models typically ranging from 50 to 100 km (Masson-Delmotte et al., 2021; Roberts et al., 2019). However, most resilience and preparedness efforts demand meteorological inputs at spatial and temporal scales much finer than the resolution of the latest GCMs (Kotamarthi et al., 2021). Consequently, current state-of-the-art GCMs still fall short in providing the fine-scale resolution required for detailed assessments in many sectors. Common approaches to addressing the scale gap between information from GCMs and the needs for actionable regional and local-scale information include statistical (Fan et al., 2013; Pierce et al., 2014) and dynamical downscaling (Prein et al., 2015; Wang and Kotamarthi, 2014, 2015; Akinsanola et al., 2024) approaches. Unlike statistical downscaling, dynamical downscaling

https://doi.org/10.5194/egusphere-2025-1112
Preprint. Discussion started: 27 March 2025

can represent a range of physical processes and their interactions within the Earth system, producing a comprehensive set of dynamically consistent high-resolution meteorological variables. The standard practice of dynamical downscaling involves the continuous operation of a regional climate model (RCM), using outputs from GCMs as initial and lateral boundary conditions. Various region-level modeling and assessment initiatives have adopted this approach, including the North American Regional Climate Change Assessment Program (Mearns et al., 2012) and the North American component of the Coordinated Regional Downscaling Experiment ~~(NA-CORDEX)~~ program (Mearns et al., 2017), demonstrating the enhanced capability to capture fine-scale features and provide more realistic and detailed projections at regional and local scales. Despite these improvements, RCMs continue to face challenges with biases arising from both their forcing data and inherent systematic errors, such as those related to model resolution, simplified physical parameterizations, and incomplete understanding of the Earth system, all of which degrade the downscaled simulations.

To address these biases and improve the reliability of future projections, various bias correction (BC) methods have been developed and employed in many studies. One of the simplest approaches is the mean-based linear scaling BC method (Tumsa, 2021). It involves calculating the difference between the mean of the historical output of the model and the mean of the observed data. The difference is then added to the future projections, scaling the model data based on the mean difference between model and observations calculated in the historical record. However, this method assumes that the relationship between model and observed data is linear with time and over the entire distribution of the variable. However, this may not capture more complex biases, especially for extreme events or in cases where the distribution of the data differs significantly between the model and observations or between the present and future projections. Furthermore, it only adjusts the mean and does not address other statistical moments, such as variability or skewness, potentially limiting its effectiveness in accurately representing the full range of weather conditions. Building on the mean-variance trend correction approach introduced by Xu and Yang (2015), Xu et al. (2021) proposed a novel bias-correction method that adjusts both the linear mean and the nonlinear variance trends in model-simulated series. The most commonly used bias-correction method, quantile mapping (QM), addresses several limitations of the mean-based linear scaling BC method by providing a more flexible and detailed approach to correcting biases in Earth systems model outputs. QM method preserves the full distribution of the data by mapping the entire cumulative distribution function (CDF) of the model data to that of the observed data. This ensures that the corrected model data reflects not just the mean, but also the variability, extremes, and other statistical characteristics of the observed data. In the QM method, a transfer function based on the quantile distribution is created by matching daily values from model simulations with observations during a reference period. This function is then applied to future model simulations. The method is typically validated by comparing bias-corrected values with observations to assess performance. Previous studies have shown that QM effectively removes biases, improving model accuracy for both mean values and extreme events (Wood, 2002; Wood et al., 2004; Boé et al., 2007; Piani et al., 2009, 2010; Ashfaq et al., 2010; Teutschbein and Seibert, 2012; Gudmundsson, 2012). However, since QM assumes that the CDF for a variable remains unchanged in future periods, it may distort signals and corrupt future trends, as the CDF is expected to shift in future projections. An alternative bias-correction method, Quantile Delta Mapping (QDM) (Cannon et al., 2015; Tong et al., 2021), improves upon QM by not only matching the CDF of modeled and observed data, but also accounting for shifts in these distributions over time, especially under future scenarios. Yet, it still assumes stationarity

https://doi.org/10.5194/egusphere-2025-1112
Preprint. Discussion started: 27 March 2025

in the quantile-based difference (delta) over time and typically does not consider the timescale-dependent nature of biases. A more detailed discussion of QM and QDM is provided in Section 2.2. Machine learning-based BC methods (Sarhadi et al., 2016; Miftahurrohmah et al., 2024; Das et al., 2022; Feng et al., 2024) have also been investigated in recent studies; however, their performance generally parallels that of quantile-based techniques and does not address the core challenge of biases that occur across multiple distinct timescales (Dhawan et al., 2024).

Indeed, biases can manifest differently at daily, monthly, seasonal, and annual scales (Haerter et al., 2011), and a correction that is effective at one timescale may fail at another and introduce inconsistencies. Although quantile-based methods like QDM can capture shifts in the overall distribution, they typically treat the data as a single timescale, thereby limiting their ability to capture biases that manifest differently across daily, monthly, seasonal, or annual timescales. Furthermore, even when acknowledging that biases may vary with timescale, isolating and representing these distinct fluctuations in the raw data is a non-trivial task. To address these gaps, we propose an **E**mpirical **M**ode **D**ecomposition-based **B**ias **C**orrection (EMDBC) framework, leveraging the adaptive nature of Empirical Mode Decomposition (EMD) (Huang et al., 1998) and its ensemble variant (EEMD) (Wu and Huang, 2009) to isolate distinct oscillatory modes at multiple timescales. By bias-correcting each extracted component (e.g., via QDM or quantile regressions) and then recombining them, EMDBC maintains key physical relationships and effectively addresses both high-frequency and low-frequency biases that conventional methods may overlook.

The remainder of this manuscript is organized as follows. Section 2 describes the experimental setup, reviews conventional BC approaches, and introduces the proposed EMDBC framework. Section 3 demonstrates EMDBC's effectiveness in a validation context and applies it to bias-correct large-scale regional Earth systems model outputs. Finally, Section 4 summarizes the findings, discusses limitations, and suggests avenues for future research.

2 Methods

2.1 Data

This study utilizes both observed and modeled temperature datasets over the continental United States to bias-correct regional-scale Earth systems model projections. The datasets are described as follows:

– **WRF-CCSM** (Wang and Kotamarthi, 2015): Building off of previous studies (Wang and Kotamarthi, 2014, 2015), this study uses moodeled 3-hourly temperature data at a 12-km spatial resolution for three time periods—historical (1995–2004), mid-century (2045–2054), and late-century (2085–2094). These projections, called WRF-CCSM, are generated by dynamically downscaling the Community Climate System Model version 4 (CCSM4) using the Weather Research and Forecasting (WRF) model version 3.3.1 (Skamarock et al., 2008). For future periods (mid-century and late-century) RCP 8.5 scenario is used. The model uses the Grell-Devenyi convective parametrization (Grell and Dévényi, 2002), the Yonsei University planetary boundary layer scheme (Noh et al., 2003), the Noah land surface model (Chen and Dudhia, 2001), the longwave and shortwave radiative schemes of the Rapid Radiation Transfer Model for GCM (Iacono et al., 2008), and the Morrison microphysics scheme (Morrison et al., 2009). Spectral nudging (Miguez-Macho et al.,

https://doi.org/10.5194/egusphere-2025-1112
Preprint. Discussion started: 27 March 2025

2004) is applied at 6-hour intervals to large-scale features, including air temperature, geopotential height, and wind, for levels above 850 hPa and wavelengths around 1200 km, using a nudging coefficient of 3x10 s^{1}. Additionally, a 1-year spin-up period is implemented to allow the model to reach equilibrium before each of the three simulations. Details on the model design and configurations are provided in Wang and Kotamarthi (2014, 2015).

– **Livneh** (Livneh et al., 2013): Observed daily temperature data at a 1/16-degree spatial resolution for the historical period (1995–2004). Livneh temperature data is generated from daily temperature observations at National Centers for Environmental Information Cooperative Observer (COOP) stations across the United States using the synergraphic mapping system (SYMAP) algorithm.

To bias-correct future regional model projections, we leverage the historical observational data (Livneh) over the period (1995–2004). The WRF-CCSM simulation spanning the same time period (historical; 1995-2004) is used to the learn the bias correction model (explained in Sections 2.2 and 2.4). Daily mean temperature data is calculated from the 3-hour outputs of WRF-CCSM to match the temporal resolution of the observed Livneh data. Similarly, the 1/16 degree Linveh data is projected onto the 12-km simulation mesh used by WRF-CCSM to match the spatial scales.

A statistical framework is then applied to identify and learn the systematic biases in the simulation data. Once trained, the bias correction model is applied to future projections for the mid-century and late-century periods. By correcting the learned biases, the model generates bias-corrected future predictions that scale more closely with observational data, thereby reducing systematic and known biases in the model output.

To assess the performance and generalizability of the proposed EMDBC method, we conducted a validation study using historical data from 1995 to 2004. This period was split into two parts: the first half (1995–1999) was used to develop and train our bias correction models, while the second half (2000–2004) was reserved for validation. The Livneh daily observed temperature series served as the reference dataset, and the EMDBC approach was applied to correct the daily temperature projections from CCSM. For a comprehensive spatial evaluation, we randomly selected seven 25×25 areas from major subregions across the continental United States, shown in Figure 1, ensuring a diverse set of conditions.

2.2 Quantile Mapping-Based Bias Adjustment

Quantile mapping (QM) is one of the most widely adopted bias correction (BC) techniques, designed to align the statistical distribution of model outputs with observations (see Chen et al. (2013) for a comprehensive review). By adjusting model outputs to match observed quantiles, QM can effectively reduce systematic biases related to both the central tendency and variability. Two prominent variants of this framework are briefly described below: Basic Quantile Mapping (QM) and Quantile Delta Mapping (QDM).

– **Basic Quantile Mapping (QM):** This approach directly corrects model outputs by aligning their quantile functions to that of the observed data. Let T_o the observed data, and T_p^{hist} the historical model simulation. For a future model output

https://doi.org/10.5194/egusphere-2025-1112
Preprint. Discussion started: 27 March 2025

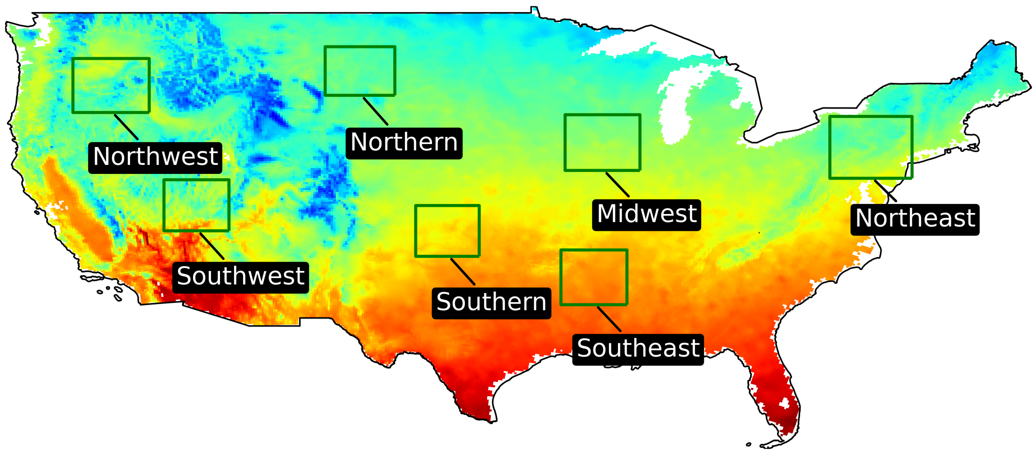

Figure 1. Map showing regions selected as case studies for validating the bias correction approaches. The base map, included only for aesthetic visual purposes, shows average WRF-CCSM temperature over the historical period (no colorbar needed).

120 T_p^{fut}, the bias-corrected value $T_p^{fut,BC}$ is given by:

$$T_p^{fut,BC} = F_o^{-1}\big(F_m^{hist}(T_p^{fut})\big), \quad (1)$$

where F_m^{hist} is the empirical CDF of the model outputs in the historical period T_p^{hist}, and F_o is the empirical CDF of the observed data T_o. Although QM ensures perfect distributional alignment for the historical period, it implicitly assumes that the observed CDF remains valid under future conditions—an assumption that can distort projected trends when the future outputs differs significantly from the historical weather regime.

– **Quantile Delta Mapping (QDM):** QDM extends QM by accounting for shifts between the historical and future model distributions. Specifically, QDM maps future values T_p^{fut} to their probabilities in both the future model CDF F_{model}^{fut} and historical model CDF F_{model}^{hist}, then determines the corresponding quantiles in the observed CDF F_o. Finally, the difference (delta) between the historical and future mappings is added to the original future values. Mathematically, it can be written as:

$$T_p^{fut,bc} = F_o^{-1}\big(F_p^{fut}(T_p^{fut})\big) + \big[T_p^{fut} - {F_p^{hist}}^{-1}\big(F_p^{fut}(T_p^{fut})\big)\big]. \quad (2)$$

This formulation permits future distributional changes to be incorporated into the bias correction.Various modifications, such as equidistant or equiratio quantile mapping (Li et al., 2010; Wang and Chen, 2014), have been shown to be mathematically equivalent to QDM (Cannon et al., 2015). In many applications involving large ranges (e.g., precipitation), the additive delta in Eq. (2) is replaced with a multiplicative factor. Nonparametric empirical CDFs are commonly used for flexibility, although parametric and semiparametric distributions can also be employed (Gudmundsson et al., 2012).

https://doi.org/10.5194/egusphere-2025-1112
Preprint. Discussion started: 27 March 2025

As highlighted in the introduction, QDM improves upon QM by allowing for distributional shifts from historical and future time periods. Nonetheless, most quantile-based methods effectively treat the entire time series on a single timescale, leaving biases at monthly, seasonal, or longer frequencies insufficiently addressed. This omission can result in residual errors that accumulate over extended periods, undermining confidence in long-term projections—a critical factor for both robust resilience assessments and strategic decision-making. These issues underscore the need for an approach that not only preserves the distributional changes in future projections but also captures timescale-dependent biases. In the next sections, we introduce the proposed EMDBC framework, which disentangles meteorological time series into their intrinsic oscillatory modes. By applying tailored bias corrections to each timescale-specific component and subsequently recombining them, EMDBC aims to overcome the core limitations of QM and QDM, thereby offering a more robust and detailed method for bias correction in future projections.

2.3 Empirical Mode Decomposition and Ensemble EMD

Empirical Mode Decomposition (EMD) (Huang et al., 1998) is a data-driven method to adaptively decompose a time series $x(t)$ into a finite set of oscillatory components, called intrinsic mode functions (IMFs), plus a residual monotonic trend. Formally, EMD expresses a time series as:

$$x(t) = \sum_{i=1}^{n} c_i(t) + r(t), \tag{3}$$

where $c_i(t)$ are the IMFs—each capturing variations over distinct timescales—and $r(t)$ is the residual. Although EMD has found utility in diverse application domains, it can suffer from *mode mixing*, where oscillations of different frequencies end up blended in a single IMF.

To address this issue, *Ensemble Empirical Mode Decomposition* (EEMD) (Wu and Huang, 2009) was introduced. EEMD adds multiple realizations of low-amplitude random noise, $\epsilon_j(t)$, to the original signal $x(t)$ to form an ensemble of signals: $x_j(t) = x(t) + \epsilon_j(t)$. EMD is then applied to each noise-added realization, and the resulting IMFs are averaged:

$$c_i^{\mathrm{EEMD}}(t) = \frac{1}{N} \sum_{j=1}^{N} c_{i,j}(t), \tag{4}$$

where $c_{i,j}(t)$ denotes the i-th IMF from the j-th noise realization, and N is the ensemble size. By smoothing over numerous noise realizations, EEMD mitigates mode mixing, yielding a more robust and interpretable decomposition. This reliability is especially valuable for timescale-specific bias correction. We use the `EEMD` function available in the Python package `PyEMD` (Laszuk, 2017) to decompose temperature signals into IMFs.

2.4 EMD-Based Bias Correction

Building on EEMD, we introduce an *Empirical Mode Decomposition-based Bias Correction* (**EMDBC**) framework aimed at rectifying model biases across multiple timescales. EMDBC is carried out in three concise steps—*(i) Timescale-wise Decomposition*, *(ii) Timescale-Specific Correction*, and *(iii) Reconstruction*—each described in detail below.

https://doi.org/10.5194/egusphere-2025-1112
Preprint. Discussion started: 27 March 2025

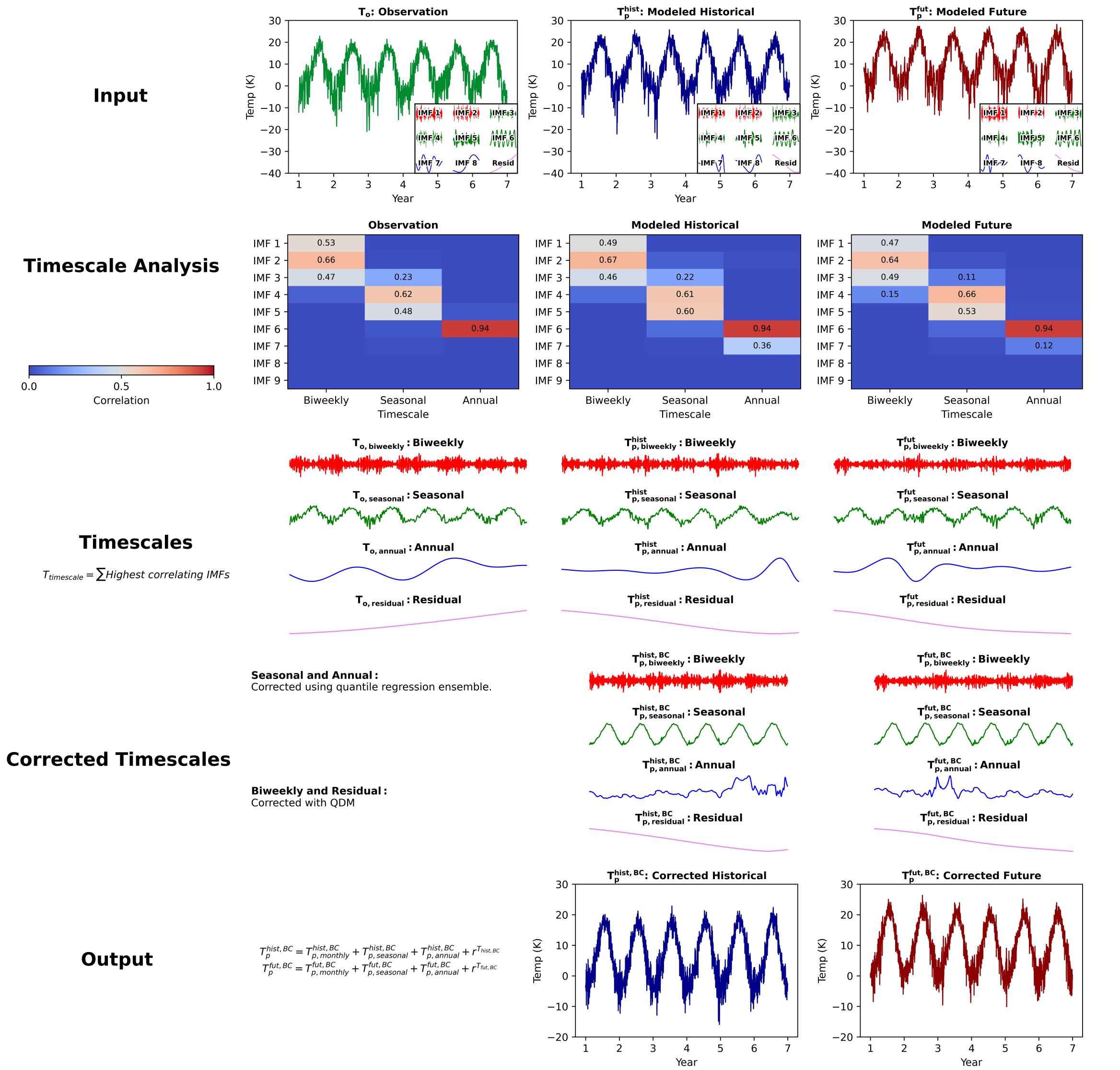

Figure 2. Timescale-wise bias correction framework using EMDBC. The input temperature series are decomposed into IMFs using EEMD. IMFs are then classified into predefined timescales: biweekly, seasonal, and annual. Bias correction is applied using QDM for biweekly timescale and residuals, and quantile regression for seasonal or annual timescales. Finally, the corrected timescales are summed to reconstruct the bias corrected temperature series.

https://doi.org/10.5194/egusphere-2025-1112
Preprint. Discussion started: 27 March 2025

2.4.1 Step 1: Timescale Decomposition

We begin by applying EEMD to decompose each time series into IMFs and a residual:

$$T_o = \sum_{j=1}^{m^{T_o}} s_j^{T_o} + r^{T_o}, \quad T_p^{\text{hist}} = \sum_{j=1}^{m^{T_p^{\text{hist}}}} s_j^{T_p^{\text{hist}}} + r^{T_p^{\text{hist}}}, \quad T_p^{\text{fut}} = \sum_{j=1}^{m^{T_p^{\text{fut}}}} s_j^{T_p^{\text{fut}}} + r^{T_p^{\text{fut}}}. \tag{5}$$

Here, T_o represents the observed series, T_p^{hist} the historical model series, and T_p^{fut} the future model series. For any given series s, the total number of extracted IMFs is m^s. Although EEMD generally reduces mode mixing, it may not fully ensure that each IMF corresponds to a unique frequency band. To address this, we implement an additional hyperparameter-tuning step that reinforces distinct frequency separation and minimizes overlap among IMFs. For the sake of clarity in presenting the timescale-wise bias correction, we have placed the detailed tuning procedure in Appendix A.

We then group these IMFs into broader frequency bands to reflect different timescales. For instance, the observed series T_o is aggregated as follows:

$$T_{o,\text{biweekly}} = \sum_{j=1}^{\lfloor \tau_1 m^{T_o} \rfloor} s_j^{T_o}, \quad T_{o,\text{seasonal}} = \sum_{j=\lfloor \tau_1 m^{T_o} \rfloor + 1}^{\lfloor \tau_2 m^{T_o} \rfloor} s_j^{T_o}, \quad T_{o,\text{annual}} = \sum_{j=\lfloor \tau_2 m^{T_o} \rfloor + 1}^{m^{T_o}} s_j^{T_o}, \tag{6}$$

where $0 < \tau_1 < \tau_2 < 1$ are thresholds (often determined via bandpass or spectral methods) that separate *biweekly*, *seasonal*, and *annual* timescales. In this study, we use the `butter` function available in scipy (Virtanen et al., 2020) to perform bandpass filtering of the original signal, isolating the frequencies associated with each timescale. We then compute correlations between each IMF and each bandpass-filtered version of the signal, selecting τ_1 and τ_2 such that the IMFs most closely matching each frequency range are grouped together. This step, illustrated in the "Timescale Analysis" portion of Figure 2, organizes the IMFs into distinct frequency bands, laying the groundwork for applying the most suitable bias-correction strategy to each timescale in the subsequent steps.

2.4.2 Step 2: Timescale-Specific Bias Correction

Although each extracted frequency band represents the same underlying variable (e.g., temperature), the nature of the biases can vary greatly depending on whether we are dealing with short-term fluctuations (e.g., biweekly scales) or longer-term patterns (e.g., seasonal or annual). To address these differences, we apply distinct bias-correction strategies tailored to each frequency band, reflecting the idea that short-term extremes and variance require different treatments from slower, more systematic drifts or trends.

Biweekly Component and Residual Trend:

At the biweekly scale, signals often exhibit substantial variability and frequent extremes, yet show little in the way of stable temporal patterns that persist across years. Because a more complex regression approach is unlikely to provide significant benefits at this resolution, we use the QDM to correct these components. Likewise, the residual term—reflecting the underlying

https://doi.org/10.5194/egusphere-2025-1112
Preprint. Discussion started: 27 March 2025

long-term trend—can also change considerably between observed and future periods. To capture these shifts and extremes effectively, we again use QDM, which directly infers quantiles from historical data while allowing for changes in the future distribution. Formally,

$$T^{\text{fut,BC}}_{p,\text{biweekly}} = \text{QDM}\big(T_{o,\text{biweekly}}, T^{\text{hist}}_{p,\text{biweekly}}, T^{\text{fut}}_{p,\text{biweekly}}\big), \tag{7}$$

$$r^{T_p^{\text{fut,BC}}} = \text{QDM}\big(r^{T_o}, r^{T_p^{\text{hist}}}, r^{T_p^{\text{fut}}}\big). \tag{8}$$

By aligning near-term fluctuations with observed quantiles, QDM preserves short-lived events and local variability without requiring additional predictors.

Seasonal and Annual Components:

At longer timescales (seasonal or annual), biases often manifest in more systematic patterns that persist across multiple years. For these scales, relying solely on QDM, an empirically driven method, may overlook structured variation better captured by predictor-based modeling. Consequently, we adopt a strategy that incorporates:

1. day: the day of the year, reflecting intra-annual variations,
2. $T^{\text{hist}}_{p,\text{long}}$: the model-simulated values aggregated at either the seasonal or annual scale, accounting for magnitude-dependent biases.

Let, $T^{\text{hist}}_{p,\text{long}} \in \{T^{\text{hist}}_{p,\text{seasonal}}, T^{\text{hist}}_{p,\text{annual}}\}$, $\quad T^{\text{fut}}_{p,\text{long}} \in \{T^{\text{fut}}_{p,\text{seasonal}}, T^{\text{fut}}_{p,\text{annual}}\}$, $\quad T_{o,\text{long}} \in \{T_{o,\text{seasonal}}, T_{o,\text{annual}}\}$, where each variable is a sum (or aggregation) of the IMFs corresponding to its relevant timescale. We define the historical bias as:

$$\text{bias}_{\text{hist}} = T^{\text{hist}}_{p,\text{long}} - T_{o,\text{long}},$$

and fit an ensemble of *quantile regressions* spanning a set of quantiles $\{q_1, q_2, \ldots, q_\ell\}$ (e.g., $q = 0.05, 0.06, \ldots, 0.99$). For each quantile q_k, we train:

$$f_{q_k}\big(\text{day}, T^{\text{hist}}_{p,\text{long}}\big) = \widehat{\text{bias}}^{(q_k)}_{\text{hist}},$$

capturing the bias at that particular quantile. The quantile regression analysis is performed using the `QuantileRegressor` model from `scikit-learn`—a Python library for machine learning (Pedregosa et al., 2011). When applied to future data, the same function yields

$$\widehat{\text{bias}}^{(q_k)}_{\text{fut}} = f_{q_k}\big(\text{day}, T^{\text{fut}}_{p,\text{long}}\big).$$

We then correct the historical and future series accordingly:

$$T^{\text{hist,BC},(q_k)}_{p,\text{long}} = T^{\text{hist}}_{p,\text{long}} - \widehat{\text{bias}}^{(q_k)}_{\text{hist}}, \quad T^{\text{fut,BC},(q_k)}_{p,\text{long}} = T^{\text{fut}}_{p,\text{long}} - \widehat{\text{bias}}^{(q_k)}_{\text{fut}}.$$

Averaging the corrections across all ℓ quantiles produces the final bias-corrected data:

$$T^{\text{hist,BC}}_{p,\text{long}} = \frac{1}{\ell}\sum_{k=1}^{\ell} T^{\text{hist,BC},(q_k)}_{p,\text{long}}, \quad T^{\text{fut,BC}}_{p,\text{long}} = \frac{1}{\ell}\sum_{k=1}^{\ell} T^{\text{fut,BC},(q_k)}_{p,\text{long}}.$$

https://doi.org/10.5194/egusphere-2025-1112
Preprint. Discussion started: 27 March 2025

By leveraging multiple predictors and quantiles, this approach better encapsulates the full distribution—from lower tails to upper extremes—while also accounting for both seasonal cycles and magnitude-dependent biases. The result is a more nuanced and robust adjustment of long-term trends than would be possible using a single-quantile or purely empirical technique. timescales.

2.4.3 Step 3: Reconstructing the Corrected Series

After bias-correcting each frequency band, we recombine them to form the final historical and future time series:

$$T_p^{\text{hist,BC}} = T_{p,\text{biweekly}}^{\text{hist,BC}} + T_{p,\text{seasonal}}^{\text{hist,BC}} + T_{p,\text{annual}}^{\text{hist,BC}} + r^{T_p,\text{BC}}, \tag{9}$$

$$T_p^{\text{fut,BC}} = T_{p,\text{biweekly}}^{\text{fut,BC}} + T_{p,\text{seasonal}}^{\text{fut,BC}} + T_{p,\text{annual}}^{\text{fut,BC}} + r^{T_p,\text{BC}}. \tag{10}$$

Here, $T_{p,\text{biweekly}}^{\text{hist,BC}}$ and $T_{p,\text{biweekly}}^{\text{fut,BC}}$ denote the QDM-corrected short-term components, while $T_{p,\text{seasonal}}^{\text{hist,BC}}$ and $T_{p,\text{annual}}^{\text{hist,BC}}$ (along with their future counterparts) correspond to the multi-quantile regression corrections at longer timescales. The residual term $r^{T_p,\text{BC}}$ is likewise corrected with QDM to address any leftover low-frequency bias.

By integrating EEMD for timescale decomposition, QDM for high-frequency biases, and multi-quantile regression for seasonal to annual scales, the **EMDBC** framework provides a flexible and robust bias-correction method. It preserves both short-term fluctuations and long-term patterns, better handles extremes, and offers a more holistic view of uncertainty — addressing some of the most pressing gaps in conventional bias-correction approaches.

2.5 Visualization

All figures were generated using the `matplotlib` Python library (Hunter, 2007).

3 Results

This section describes the results from the validation study on seven case study areas and over the full domain. In both validation and full domain results, we apply a spatial smoothing procedure to the bias corrected daily temperature fields for both methods (QDM and EMDBC), while also censoring any values that exceed the original model's range to ensure numerical consistency and prevent unrealistic outliers. Since temperature typically exhibits strong spatial coherence, correcting each grid cell independently can introduce small-scale inconsistencies or artifacts. By averaging each cell's value with those of its immediate neighbors in a small $2D$ window (a 3×3 window in our experiments), we enhance local spatial continuity while preserving the broader-scale features necessary for downstream impact analyses.

3.1 Validation results

Here, we include a comprehensive evaluation of traditional bias correction methods alongside our proposed approach. By applying the bias correction models to both the historical training scenario and the historical validation scenario, we can

https://doi.org/10.5194/egusphere-2025-1112
Preprint. Discussion started: 27 March 2025

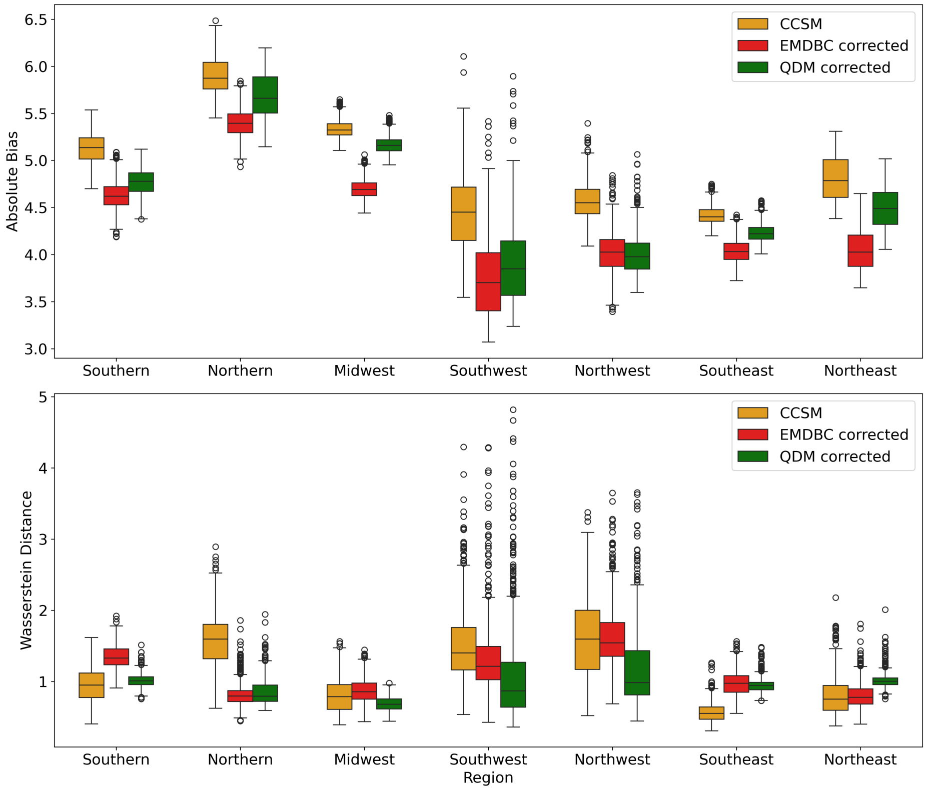

Figure 3. Comparison of Absolute Biases and Wasserstein Distances Across Sub-Regions. Top: Boxplots of the absolute temperature bias for the original (CCSM) and bias-corrected (EMDBC and QDM) simulations across sub-regions on the validation dataset. **Bottom:** Boxplots of the corresponding Wasserstein distances between the observed and modeled temperature distributions across sub-regions on the validation dataset.

effectively assess each models ability to address biases and generalize across temporal scales where observed data doesn't exist (i.e., the future mid- and late century scenarios).

We implement QDM and the proposed EMDBC to bias-correct the validation dataset introduced in Section 2.1.Figure 3 top panel shows the spatial distribution of the average absolute bias across these subregions and highlights the consistent performance gains achieved by EMDBC on held-out validation data. In addition, we examined the distributional similarity of the observed series and the model-projected series (both before and after bias correction) using the Wasserstein distance (WD). Figure 3 down panel illustrates the WD across all subregions, demonstrating that the EMDBC correction preserves a distributional similarity to the observed series comparable to the QDM approach.

Next, we evaluated the performance of EMDBC at four distinct timescales—biweekly, monthly, seasonal, and half-annual—by comparing it to both QDM and the original CCSM output. To focus on each timescale, we used an FFT-based bandpass filtering method. First, the daily temperature series were transformed into the frequency domain. Then, all frequencies outside

https://doi.org/10.5194/egusphere-2025-1112
Preprint. Discussion started: 27 March 2025

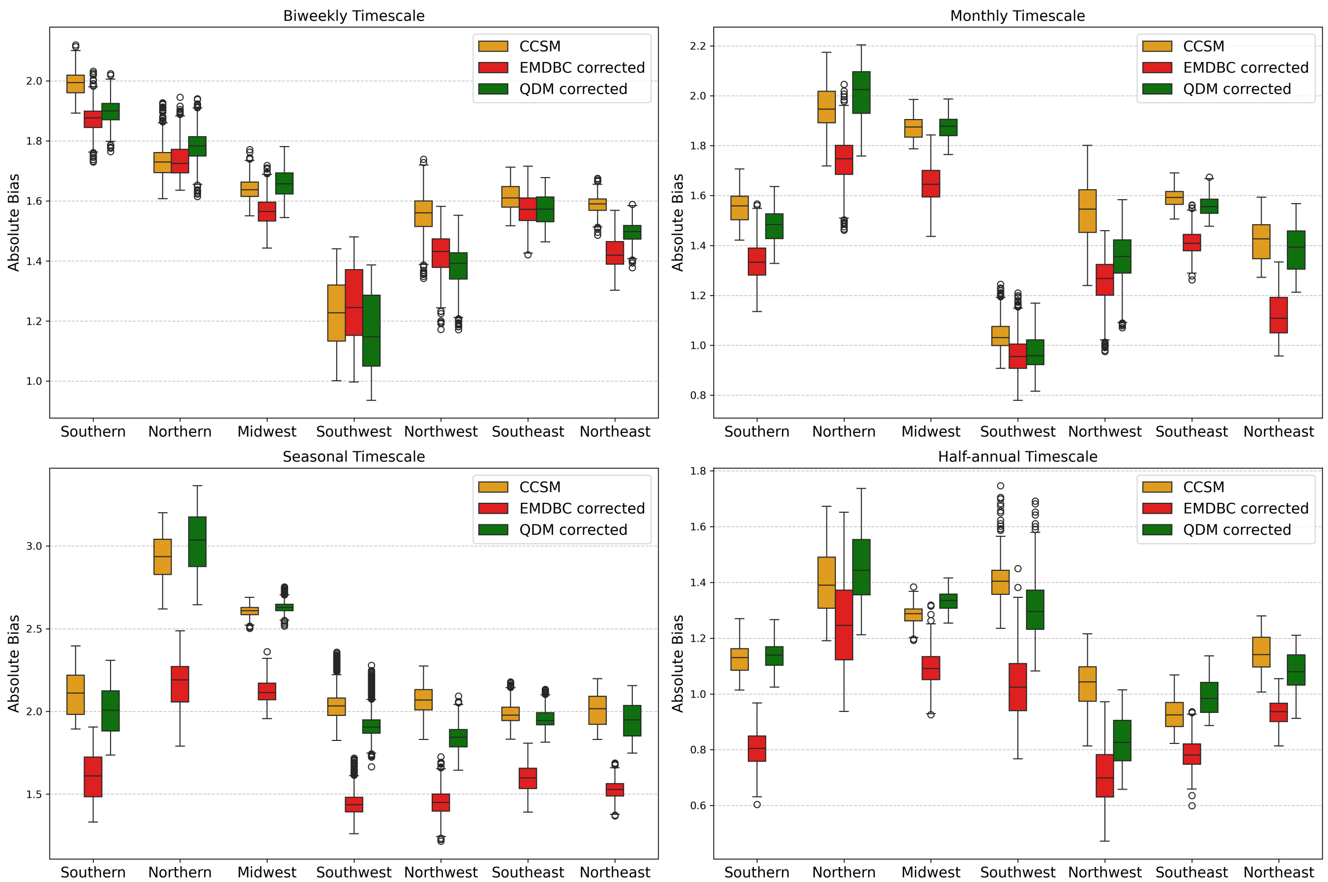

Figure 4. The timescale wise average absolute bias per subregion on the validation dataset.

the target range were set to zero before an inverse transform was applied to reconstruct the filtered signal. This approach allowed us to isolate and compare how effectively each bias correction method captures variability at different temporal scales. Figure 4 shows the spatial distribution of the absolute bias across subregions for each filtered timescale. While EMDBC and QDM perform comparably at shorter timescales (biweekly), EMDBC demonstrates a progressively closer alignment with the observed series at longer timescales (monthly, seasonal, half-annual). Accurate bias correction at coarser temporal resolutions is especially important for large-scale resilience assessments and long-term planning, where cumulative effects and extended trends play a crucial role. This includes common uses cases of RCM and GCM, such as global, national, or regional impact studies (USGCRP, 2023); policy planning for risk assessment (Ranasinghe et al., 2021); energy infrastructure trends for long-term heating or cooling demands (Tan et al., 2023); drought security (Gamelin et al., 2022); agriculture planning (Jin et al., 2017); and understanding ecosystem biodiversity shifts (Liu et al., 2025). In other words, EMDBC shows promising ability to reduce temperature trend distortion caused by systematic biases due to model uncertainties and better capture temperature

https://doi.org/10.5194/egusphere-2025-1112
Preprint. Discussion started: 27 March 2025

trend dynamics. This improved ability to preserve these longer-term patterns makes it a more reliable choice than QDM for applications that depend on consistent performance across multiple timescales.

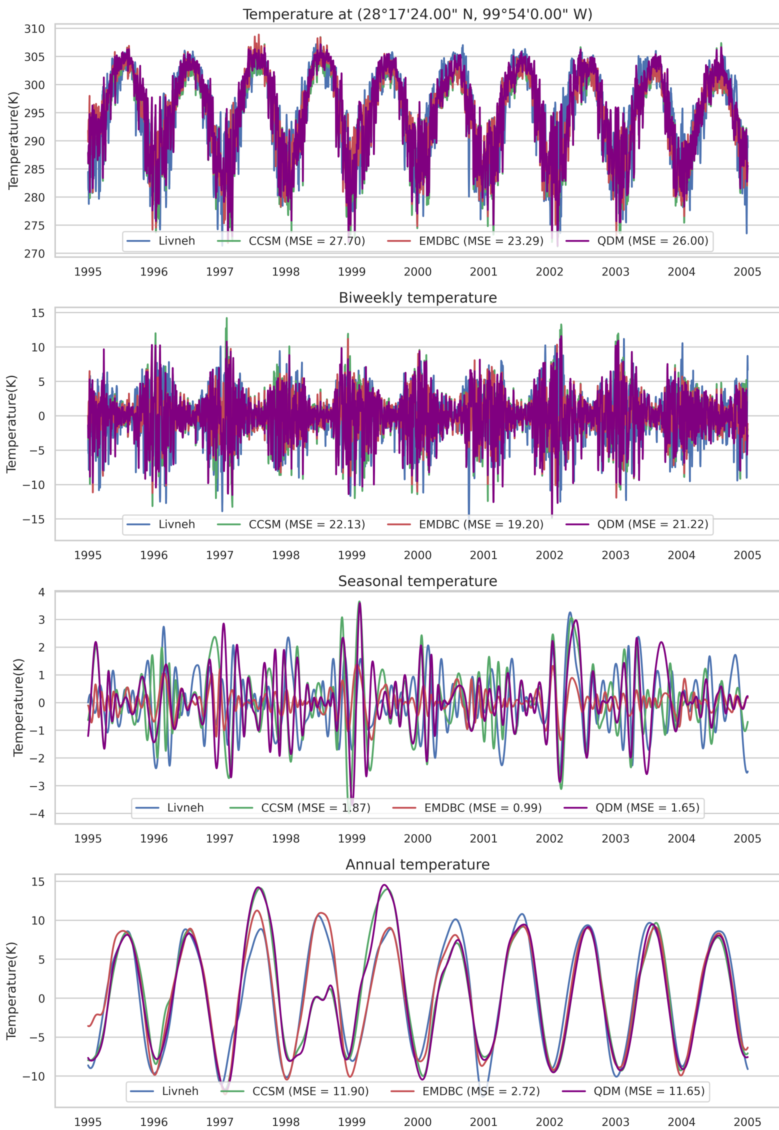

Figure 5. Illustration of bias correction across multiple timescales. At a sample location, we show the observed Livneh data, the raw CCSM projection, and the corresponding bias-corrected series from EMDBC and QDM, each decomposed using the EMD-based method described in Section 2.4. While QDM achieves performance comparable to EMDBC at the daily (training) scale, EMDBC more accurately preserves the broader trajectory of the observed series across seasonal and annual timescales.

https://doi.org/10.5194/egusphere-2025-1112
Preprint. Discussion started: 27 March 2025

275 These results demonstrate that EMDBC successfully preserves bias-corrected signals over a broad range of temporal frequencies. By confirming EMDBC's effectiveness in an out-of-sample setting in this validation experiment, we gain confidence that it retains crucial physical relationships within the model more effectively than the traditional QDM, particularly at longer timescales. In the next section, we will evaluate its performance on the full GCM domain.

3.2 Over full domain

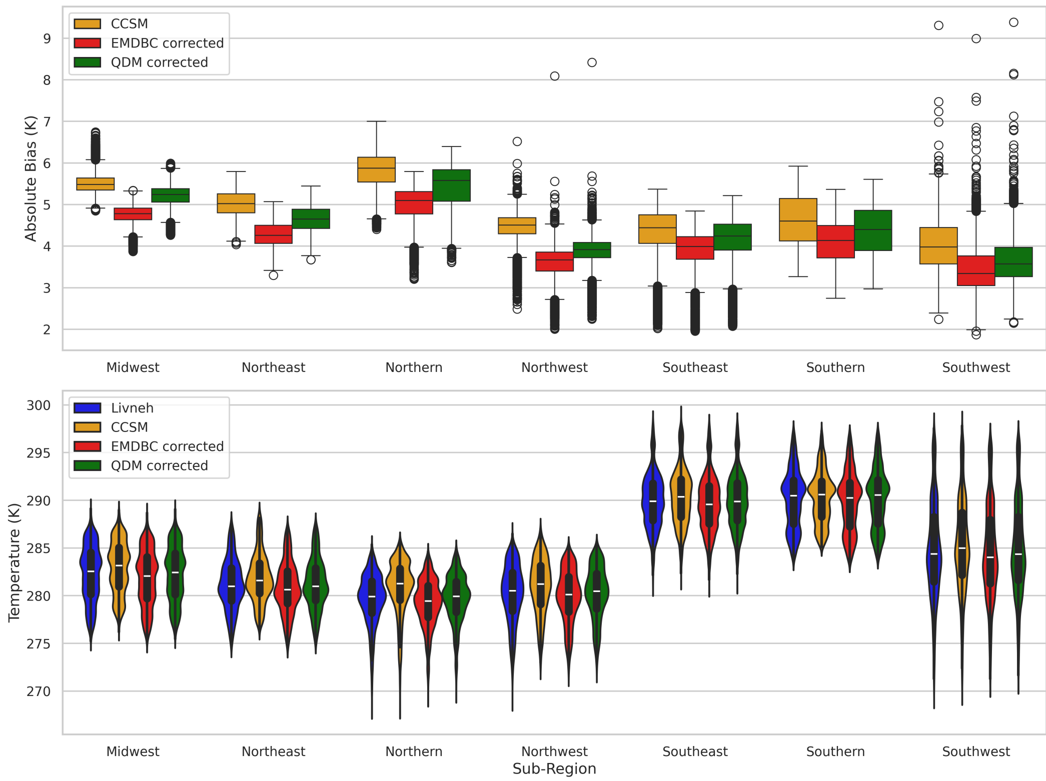

Figure 6. Comparison of CCSM Temperature Biases and Temperature Distributions Across Sub-Regions. Top: Boxplots of the absolute temperature bias before and after applying EMDBC and QDM corrections. **Bottom:** Violin plots showing the distribution of the average temperature for each sub-region.

280 We apply EMDBC and QDM to the expanded model domain—covering all relevant time periods—to illustrate each method's impact on temperature bias correction. As an initial illustration, Figure 5 presents a single sampled location, decomposed in multiple timescales via the EMD-based approach described in Section 2.4. While QDM and EMDBC both perform well at the daily (training) scale, EMDBC more accurately preserves the longer-term fluctuations (e.g., seasonal and annual) seen in the observed Livneh data.

https://doi.org/10.5194/egusphere-2025-1112
Preprint. Discussion started: 27 March 2025

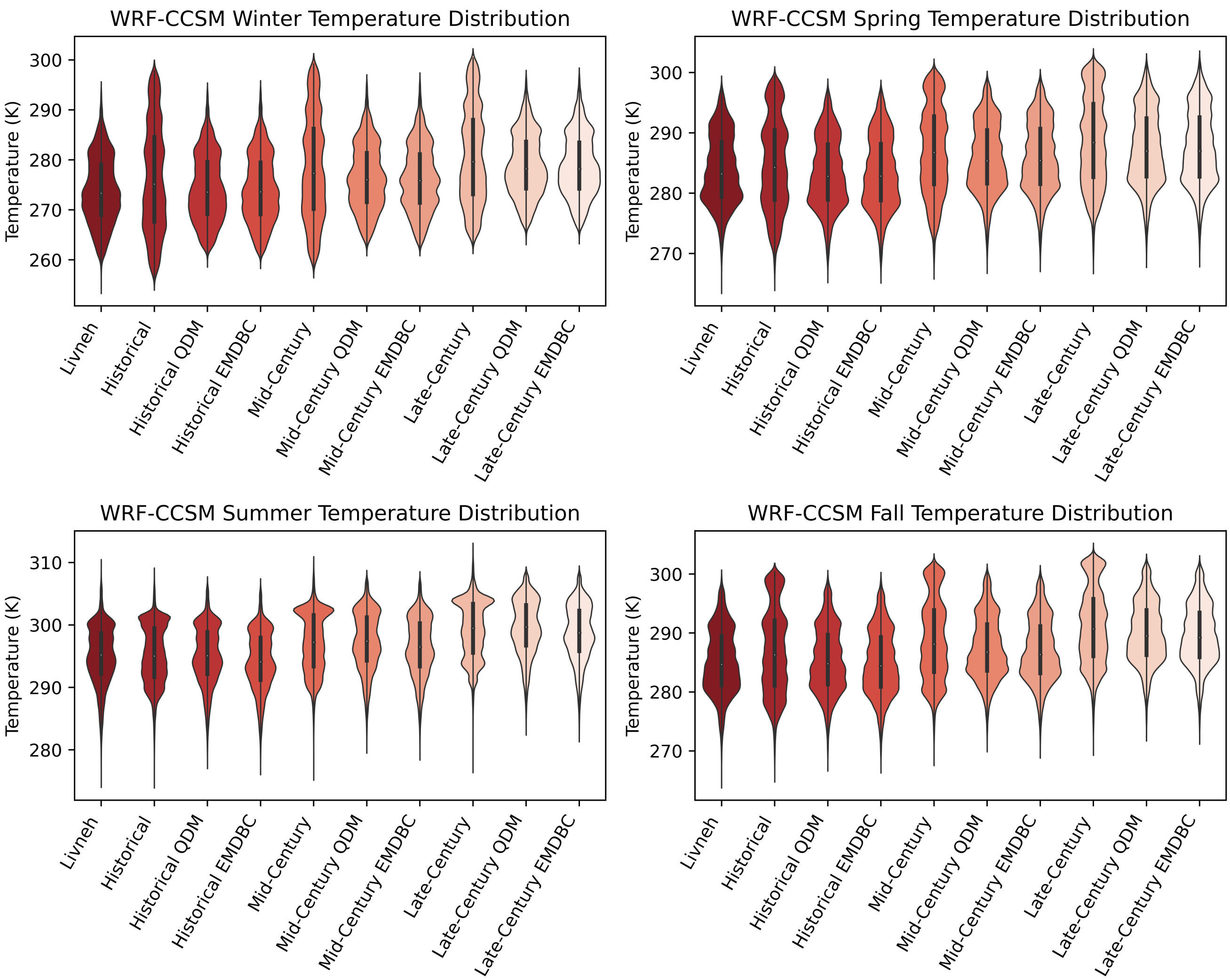

Figure 7. The mean daily temperature by season (winter, spring, summer, fall) across Livneh and WRF-CCSM timeframes before and after bias correction. Results for QDM and EMDBC are included.

https://doi.org/10.5194/egusphere-2025-1112
Preprint. Discussion started: 27 March 2025

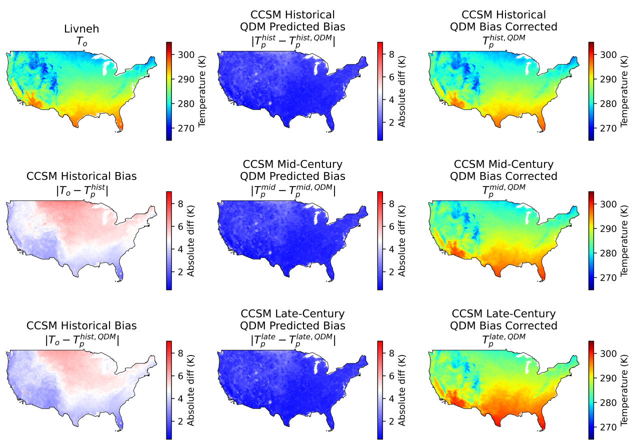

Figure 8. Temperature and temperature bias comparisons over CONUS before and after applying QDM. **Left:** Observed temperature (Livneh), WRF-CCSM average daily absolute bias, and QDM-corrected WRF-CCSM average daily absolute bias. **Middle:** Magnitude of QDM correction in historical, mid-century, and late-century timeframes. **Right:** QDM-corrected temperatures for WRF-CCSM historical, mid-century, and late-century periods.

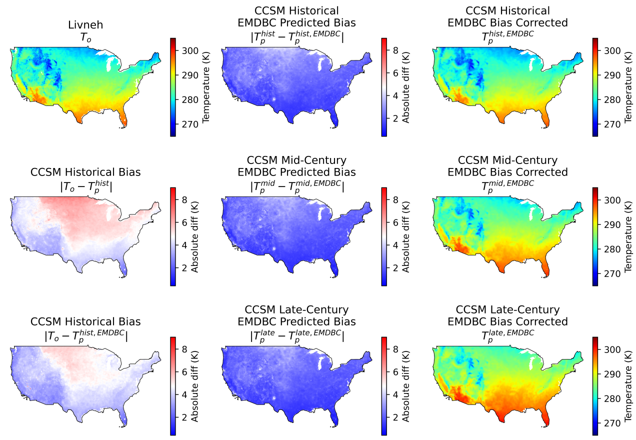

Figure 9. Temperature and temperature bias comparisons over CONUS before and after applying EMDBC. **Left:** Observed temperature (Livneh), WRF-CCSM average daily absolute bias, and EMDBC-corrected WRF-CCSM average daily absolute bias. **Middle:** Magnitude of EMDBC correction in historical, mid-century, and late-century timeframes. **Right:** EMDBC-corrected temperatures for WRF-CCSM historical, mid-century, and late-century periods.

Turning next to broader spatial analyses, Figure 6 focuses on various sub-regions across CONUS. In each sub-region, the top panel compares the absolute temperature bias between the model projected and the observed series before and after correction with EMDBC and QDM, whereas the right panel shows the distribution of the average temperature. This figure demonstrates that EMDBC consistently reduces biases while maintaining an overall temperature distribution comparable to QDM.

To verify whether these distributional consistencies hold across individual seasons, we next analyze Figure 7, which illustrates the spatial distribution of seasonal-average temperature for the Livneh observations, the raw WRF-CCSM outputs, and their bias-corrected counterparts. At this aggregated seasonal level, both EMDBC and QDM move the model's temperature distribution closer to the observed data while retaining the overall projected warming trends through the mid- and late-century timeframes. This consistency further suggests that EMDBC not only reduces bias magnitude but also closely matches observed seasonal temperature patterns.

Finally, Figures 9 and 8 show the predicted daily bias and the corresponding spatial maps (e.g., annual or multi-year averages) for the raw and bias-corrected WRF-CCSM outputs. Here, "predicted bias" refers to the difference between the modeled temperature and its bias-corrected counterpart. EMDBC generally applies a stronger correction than QDM, resulting in slightly cooler daily temperature fields and a more uniform reduction of bias across the domain. Although we cannot fully validate

https://doi.org/10.5194/egusphere-2025-1112
Preprint. Discussion started: 27 March 2025

future-period corrections in the absence of observations, EMDBC's stronger alignment with historical data and its lower bias in validation sub-regions (Section 3.1) suggest it is well-equipped to handle changing conditions while preserving both short- and long-term temperature variability.

4 Conclusion

This study applies the EMDBC framework to the daily temperature outputs of regional scale dynamically downscaling output developed using the WRF model. Downscaled output using WRF and the CCSM model for the CMIP5 respoistory, WRF-CCSM, at three time periods (historical, mid-century, and late-century) were used for the study. Furthermore, the EMDBC approach is validated by splitting historical model and observed data into training and validation sets and evaluating the validation set for bias reduction. In order to demonstrate the benefits of EMDBC, we compare the distributional similarities and absolute bias at varying timescales of the observed, model-projected, and bias corrected series. The results of this study highlight the importance of addressing biases across multiple timescales when correcting regional Earth systems model outputs. Conventional approaches, such as mean-based linear scaling or quantile mapping, often focus on single distributions without adequately capturing longer-term fluctuations (e.g., monthly or seasonal). This limitation can lead to distorted trends and weakened physical consistency among meteorological variables, thereby reducing confidence in model projections used for impact assessments and decision-making. In contrast, our EMDBC framework leverages Empirical Mode Decomposition (EMD) to isolate and correct distinct timescale wise oscillatory decomposition of a given signal, thereby preserving both short-term and long-term variability. Validation experiments show that EMDBC aligns better with observations at coarser temporal resolutions compared to conventional approaches, ensuring more accurate trends and enhanced physical consistency. These improvements are particularly relevant for applications where long-term signals—such as drought monitoring and risk assessment—play a critical role.

Nonetheless, several limitations remain. While the EMD decomposition offers theoretical guarantees for extracting intrinsic modes, segmenting them into discrete timescales still depends on user-defined thresholds, introducing a degree of subjectivity. A more rigorous, automated framework for determining these boundaries would further bolster EMDBC's robustness. Additionally, although ensemble EMD (EEMD) helps mitigate mode mixing, more advanced signal-processing or machine learning techniques could optimize the decomposition process. Another promising avenue for future work is the exploration of multivariate EMD approaches, which would facilitate a more comprehensive bias correction by preserving inter-variable dependencies among variable fields. Despite these open questions, our results demonstrate that a timescale-aware bias-correction strategy significantly enhances model projection reliability and paves the way for continued innovation in this area.

Code and data availability

All Python scripts for the Empirical Mode Decomposition-based Bias Correction (EMDBC) are available in Argonne's GitLab repository at: https://git.cels.anl.gov/jfeinstein/emdbc-paper (Feinstein, 2025). This repository also includes time series data

https://doi.org/10.5194/egusphere-2025-1112
Preprint. Discussion started: 27 March 2025

for the seven 25×25 validation areas selected from major subregions of the continental United States (Figure 1), encompassing Livneh observations and WRF-CCSM simulations. The full-domain WRF-CCSM model summaries are provided via the ClimRR portal at: https://climrr.anl.gov/ (Argonne National Laboratory, 2025), which hosts regional climate projections for the entire United States.

Appendix A: Optimal Tuning of IMFs for EMDBC

The performance of the proposed EMDBC framework depends on the quality and separation of the IMFs generated during the decomposition process. A common challenge in EMD methods is *mode-mixing*, where oscillatory modes of different frequencies are entangled within a single IMF, reducing interpretability and effectiveness (Tang et al., 2012). While the Ensemble EMD (EEMD) approach (Wu and Huang, 2009) mitigates mode-mixing by introducing random noise, it does not fully eliminate the issue. Several alternative strategies have been proposed to ensure distinct frequency bands for IMFs (Tang et al., 2012; Fosso and Molinas, 2018), but none has proven universally robust.

To address the instability of IMFs and ensure their meaningful separation across timescales, we impose constraints on their *maximum amplitude frequencies* (f_{max}) calculated using the Fast Fourier Transform (FFT) (Rockmore, 2000). This process is iterative: IMFs are generated, evaluated against the constraints, and refined until all conditions are satisfied. The constraints are defined as follows:

- **Ensuring Distinct Timescales:** Each IMF must represent a unique timescale, maintaining a strictly decreasing frequency trend:

  $$\Delta f_{\text{max}}^{(j)} = f_{\text{max}}^{(j)} - f_{\text{max}}^{(j+1)} > 0, \quad \forall j,$$

  where $f_{\text{max}}^{(j)}$ denotes the maximum amplitude frequency of the j-th IMF.

- **Preventing Overlap:** To avoid redundancy, the relative change in frequency between consecutive IMFs must exceed a minimum threshold:

  $$\frac{\Delta f_{\text{max}}^{(j)}}{f_{\text{max}}^{(j)}} > \delta_{\text{min}}.$$

- **Maintaining Regularity:** The progression of frequencies across IMFs should be smooth, avoiding abrupt changes. This is enforced by ensuring:

  $$\frac{\Delta f_{\text{max}}^{(j)}}{f_{\text{max}}^{(j)}} < \delta_{\text{max}}.$$

The thresholds δ_{min} and δ_{max} act as hyperparameters, which can be tuned through cross-validation. In our experiments, setting $\delta_{\text{min}} = 0.2$ and $\delta_{\text{max}} = 0.8$ yielded satisfactory results. The algorithm iteratively checks these constraints after each generation of IMFs. If all conditions are satisfied, the process terminates; otherwise, new IMFs are generated, and the constraints are re-evaluated. The following algorithm outlines the major steps in this iterative optimization process:

https://doi.org/10.5194/egusphere-2025-1112
Preprint. Discussion started: 27 March 2025

Algorithm A1 Iterative Optimization of IMFs for EMDBC

```
Input: Time series x(t), thresholds δ_min, δ_max
Output: Optimized set of IMFs, {s_j}_{j=1}^m
Initialize: Generate initial IMFs using EEMD: {s_j}_{j=1}^m
Compute maximum amplitude frequencies f_max^(j) using FFT
while any constraint is violated do
    Check distinct timescales: Δf_max^(j) > 0, ∀j
    Check overlap: Δf_max^(j) / f_max^(j) > δ_min
    Check regularity: Δf_max^(j) / f_max^(j) < δ_max
    if any condition is violated then
        Regenerate IMFs using updated parameters
        Recompute f_max^(j)
    end if
end while
return Optimized {s_j}_{j=1}^m
```

By iteratively applying these constraints, we ensure that the IMFs represent distinct timescales, avoid redundancy, and maintain smooth frequency progression. This optimization significantly enhances the stability of the decomposition and improves the effectiveness of EMDBC in handling challenging cases of mode-mixing or overlapping frequency bands.

Author contributions. **Conceptualization, Formal analysis, Validation, Visualization**: AG, JF; **Data curation, Investigation, Software**: AG, JF, CA; **Funding acquisition, Resources, Supervision**: RK, TW; **Methodology**: AG, JF, IR, AA, WH; **Project administration**: RK, TW, JB; **Writing – original draft**: AG, JF, CJ; **Writing – review & editing**: AG, JF, IR, AA, CA, CJ, JB, TW, WH, RK.

Competing interests. The authors declare that they have no competing interests.

Acknowledgements. Argonne National Laboratory's contribution is based upon work supported by Laboratory Directed Research and Development (LDRD) funding from Argonne National Laboratory, provided by the Director, Office of Science, of the U.S. Department of Energy under Contract No. DE-AC02-06CH11357. The training was conducted on the Bebop and Improv CPU clusters at the Laboratory Computing Resource Center (LCRC) of Argonne National Laboratory. We would like to acknowledge the use of OpenAI's ChatGPT and DeepSeek's models for assistance in code development and figure generation.

https://doi.org/10.5194/egusphere-2025-1112
Preprint. Discussion started: 27 March 2025

References

Akinsanola, A. A., Jung, C., Wang, J., and Kotamarthi, V. R. (2024). Evaluation of precipitation across the contiguous united states, alaska, and puerto rico in multi-decadal convection-permitting simulations. *Scientific Reports*, 14(1):1238.

Argonne National Laboratory (2025). Climrr. temperature datasets. https://climrr.anl.gov/.

Ashfaq, M., Bowling, L. C., Cherkauer, K., Pal, J. S., and Diffenbaugh, N. S. (2010). Influence of climate model biases and daily-scale temperature and precipitation events on hydrological impacts assessment: a case study of the united states. *Journal of Geophysical Research*, 115:D14.

Boé, J., Terray, L., Habets, F., and Martin, E. (2007). Statistical and dynamical downscaling of the seine basin climate for hydro-meteorological studies. *International Journal of Climatology*, 27:1643–1655.

Cannon, A. J., Sobie, S. R., and Murdock, T. Q. (2015). Bias correction of gcm precipitation by quantile mapping: how well do methods preserve changes in quantiles and extremes? *Journal of Climate*, 28(17):6938–6959.

Chen, F. and Dudhia, J. (2001). Coupling an advanced land surface–hydrology model with the penn state–ncar mm5 modeling system. part i: Model implementation and sensitivity. *Monthly Weather Review*, 129(4):569 – 585.

Chen, J., Brissette, F. P., Chaumont, D., and Braun, M. (2013). Finding appropriate bias correction methods in downscaling precipitation for hydrologic impact studies over north america. *Water Resources Research*, 49(7):4187–4205.

Das, P., Zhang, Z., and Ren, H. (2022). Evaluation of four bias correction methods and random forest model for climate change projection in the mara river basin, east africa. *Journal of Water and Climate Change*, 13(4):1900–1919.

Dhawan, P., Dalla Torre, D., Niazkar, M., Kaffas, K., Larcher, M., Righetti, M., and Menapace, A. (2024). A comprehensive comparison of bias correction methods in climate model simulations: Application on era5-land across different temporal resolutions. *Heliyon*, 10(23):e40352.

Fan, L., Chen, D., Fu, C., et al. (2013). Statistical downscaling of summer temperature extremes in northern china. *Advances in Atmospheric Sciences*, 30:1085–1095.

Feinstein, J. (2025). EMDBC-Paper Repository. https://git.cels.anl.gov/jfeinstein/emdbc-paper. [Accessed 1 March 2025].

Feng, S., Tan, Y., Kang, J., Zhong, Q., Li, Y., and Ding, R. (2024). Bias correction of tropical cyclone intensity for ensemble forecasts using the xgboost method. *Weather and Forecasting*, 39(2):323–332.

Fosso, O. B. and Molinas, M. (2018). Emd mode mixing separation of signals with close spectral proximity in smart grids. In *2018 IEEE PES Innovative Smart Grid Technologies Conference Europe (ISGT-Europe)*, pages 1–6.

Gamelin, B. L., Feinstein, J., Wang, J., Bessac, J., Yan, E., and Kotamarthi, V. R. (2022). Projected U.S. drought extremes through the twenty-first century with vapor pressure deficit. *Sci. Rep.*, 12(1):8615.

Grell, G. A. and Dévényi, D. (2002). A generalized approach to parameterizing convection combining ensemble and data assimilation techniques. *Geophysical Research Letters*, 29(14):38–1–38–4.

Gudmundsson, L. (2012). qmap: Statistical transformations for postprocessing climate model output. R package version 1.0–3. Available online at https://cran.r-project.org/web/packages/qmap/.

Gudmundsson, L., Bremnes, J. B., Haugen, J. E., and Engen-Skaugen, T. (2012). Downscaling rcm precipitation to the station scale using statistical transformations–a comparison of methods. *Hydrology and Earth System Sciences*, 16(9):3383–3390.

Haerter, J. O., Hagemann, S., Moseley, C., and Piani, C. (2011). Climate model bias correction and the role of timescales. *Hydrology and Earth System Sciences*, 15(3):1065–1079.

https://doi.org/10.5194/egusphere-2025-1112
Preprint. Discussion started: 27 March 2025

Huang, N. E., Shen, Z., Long, S. R., Wu, M. C., Shih, H. H., Zheng, Q., Yen, N.-C., Tung, C. C., and Liu, H. H. (1998). The empirical mode decomposition and the hilbert spectrum for nonlinear and non-stationary time series analysis. *Proceedings of the Royal Society of London. Series A: mathematical, physical and engineering sciences*, 454(1971):903–995.

Hunter, J. D. (2007). Matplotlib: A 2d graphics environment. *Computing in Science & Engineering*, 9(3):90–95.

Iacono, M. J., Delamere, J. S., Mlawer, E. J., Shephard, M. W., Clough, S. A., and Collins, W. D. (2008). Radiative forcing by long-lived greenhouse gases: Calculations with the AER radiative transfer models. *Journal of Geophysical Research*, 113:D13103.

Jin, Z., Zhuang, Q., Wang, J., Archontoulis, S. V., Zobel, Z., and Kotamarthi, V. R. (2017). The combined and separate impacts of climate extremes on the current and future US rainfed maize and soybean production under elevated CO2. *Glob. Chang. Biol.*, 23(7):2687–2704.

Kotamarthi, R. et al. (2021). *Downscaling Techniques for High-Resolution Climate Projections: From Global Change to Local Impacts*. Cambridge University Press, Cambridge.

Laszuk, D. (2017). Python implementation of empirical mode decomposition algorithm. https://github.com/laszukdawid/PyEMD.

Li, H., Sheffield, J., and Wood, E. F. (2010). Bias correction of monthly precipitation and temperature fields from intergovernmental panel on climate change ar4 models using equidistant quantile matching. *Journal of Geophysical Research: Atmospheres*, 115(D10).

Liu, J., Kyle, C., Wang, J., Kotamarthi, R., Koval, W., Dukic, V., and Dwyer, G. (2025). Climate change drives reduced biocontrol of the invasive spongy moth. *Nat. Clim. Chang.*, 15(2):210–217.

Livneh, B., Rosenberg, E. A., Lin, C., Nijssen, B., Mishra, V., Andreadis, K. M., Maurer, E. P., and Lettenmaier, D. P. (2013). A long-term hydrologically based dataset of land surface fluxes and states for the conterminous united states: Update and extensions. *Journal of Climate*, 26(23):9384 – 9392.

Masson-Delmotte, V., Zhai, P., Pirani, A., Connors, S., Péan, C., Berger, S., Caud, N., Chen, Y., Goldfarb, L., Gomis, M., Huang, M., Leitzell, K., Lonnoy, E., Matthews, J., Maycock, T., Waterfield, T., Yelekçi, O., Yu, R., and Zhou, B., editors (2021). *Climate Change 2021: The Physical Science Basis. Contribution of Working Group I to the Sixth Assessment Report of the Intergovernmental Panel on Climate Change*. Cambridge University Press, Cambridge, United Kingdom and New York, NY, USA.

Mearns, L. O., Arritt, R., Biner, S., Bukovsky, M. S., McGinnis, S., Sain, S., Caya, D., Correia, J., Flory, D., Gutowski, W., Takle, E. S., Jones, R., Leung, R., Moufouma-Okia, W., McDaniel, L., Nunes, A. M. B., Qian, Y., Roads, J., Sloan, L., and Snyder, M. (2012). The north american regional climate change assessment program: Overview of phase i results. *Bulletin of the American Meteorological Society*, 93(9):1337 – 1362.

Mearns, L. O. et al. (2017). The na-cordex dataset, version 1.0. Accessed [date].

Miftahurrohmah, B., Kuswanto, H., Pambudi, D. S., Fauzi, F., and Atmaja, F. (2024). Assessment of the support vector regression and random forest algorithms in the bias correction process on temperatures. *Procedia Computer Science*, 234:637–644.

Miguez-Macho, G., Stenchikov, G. L., and Robock, A. (2004). Spectral nudging to eliminate the effects of domain position and geometry in regional climate model simulations. *Journal of Geophysical Research: Atmospheres*, 109.

Morrison, H., Thompson, G., and Tatarskii, V. (2009). Impact of cloud microphysics on the development of trailing stratiform precipitation in a simulated squall line: Comparison of one- and two-moment schemes. *Monthly Weather Review*, 137:991–1007.

Noh, Y., Cheon, W. G., Hong, S. Y., and et al. (2003). Improvement of the K-profile model for the planetary boundary layer based on large eddy simulation data. *Boundary-Layer Meteorology*, 107:401–427.

Pedregosa, F., Varoquaux, G., Gramfort, A., Michel, V., Thirion, B., Grisel, O., Blondel, M., Prettenhofer, P., Weiss, R., Dubourg, V., Vanderplas, J., Passos, A., Cournapeau, D., Brucher, M., Perrot, M., and Duchesnay, E. (2011). Scikit-learn: Machine learning in Python. *Journal of Machine Learning Research*, 12:2825–2830.

https://doi.org/10.5194/egusphere-2025-1112
Preprint. Discussion started: 27 March 2025

Piani, C., Haerter, J. O., and Coppola, E. (2009). Statistical bias correction for daily precipitation in regional climate models over europe. *Theoretical and Applied Climatology*, 99(1–2):187–192.

Piani, C., Weedon, G. P., Best, M., Gomes, S. M., Viterbo, P., Hagemann, S., and Haerter, J. O. (2010). Statistical bias correction of global simulated daily precipitation and temperature for the application of hydrological models. *Journal of Hydrology*, 395(3–4):199–215.

Pierce, D. W., Cayan, D. R., and Thrasher, B. L. (2014). Statistical downscaling using localized constructed analogs (loca). *Journal of hydrometeorology*, 15(6):2558–2585.

Prein, A. F., Langhans, W., Fosser, G., Ferrone, A., Ban, N., Goergen, K., Keller, M., Tölle, M., Gutjahr, O., Feser, F., Brisson, E., Kollet, S., Schmidli, J., van Lipzig, N. P. M., and Leung, R. (2015). A review on regional convection-permitting climate modeling: Demonstrations, prospects, and challenges. *Reviews of Geophysics*, 53(2):323–361.

Ranasinghe, R., Ruane, A., Vautard, R., Arnell, N., Coppola, E., Cruz, F., Dessai, S., Islam, A., Rahimi, M., Ruiz Carrascal, D., Sillmann, J., Sylla, M., Tebaldi, C., Wang, W., and Zaaboul, R. (2021). Climate change information for regional impact and for risk assessment. In Masson-Delmotte, V., Zhai, P., Pirani, A., Connors, S., Péan, C., Berger, S., Caud, N., Chen, Y., Goldfarb, L., Gomis, M., Huang, M., Leitzell, K., Lonnoy, E., Matthews, J., Maycock, T., Waterfield, T., Yelekçi, O., Yu, R., and Zhou, B., editors, *Climate Change 2021: The Physical Science Basis. Contribution of Working Group I to the Sixth Assessment Report of the Intergovernmental Panel on Climate Change*, pages 1767–1926. Cambridge University Press.

Roberts, M. J., Baker, A., Blockley, E. W., Calvert, D., Coward, A., Hewitt, H. T., Jackson, L. C., Kuhlbrodt, T., Mathiot, P., Roberts, C. D., Schiemann, R., Seddon, J., Vannière, B., and Vidale, P. L. (2019). Description of the resolution hierarchy of the global coupled hadgem3-gc3.1 model as used in cmip6 highresmip experiments. *Geoscientific Model Development*, 12(12):4999–5028.

Rockmore, D. (2000). The fft: an algorithm the whole family can use. *Computing in Science Engineering*, 2(1):60–64.

Sarhadi, A., Burn, D. H., Johnson, F., Mehrotra, R., and Sharma, A. (2016). Water resources climate change projections using supervised nonlinear and multivariate soft computing techniques. *Journal of Hydrology*, 536:119–132.

Skamarock, W., Klemp, J., Dudhia, J., Gill, D. O., Barker, D., Duda, M. G., Huang, X.-Y., Wang, W., and Powers, J. G. (2008). A description of the advanced research WRF version 3. Technical report, University Corporation for Atmospheric Research.

Tan, H., Kotamarthi, R., Wang, J., Qian, Y., and Chakraborty, T. C. (2023). Impact of different roofing mitigation strategies on near-surface temperature and energy consumption over the chicago metropolitan area during a heatwave event. *Sci. Total Environ.*, 860(160508):160508.

Tang, B., Dong, S., and Song, T. (2012). Method for eliminating mode mixing of empirical mode decomposition based on the revised blind source separation. *Signal Processing*, 92(1):248–258.

Teutschbein, C. and Seibert, J. (2012). Bias correction of regional climate model simulations for hydrological climate-change impact studies: review and evaluation of different methods. *Journal of Hydrology*, 456–457:12–29.

Tong, Y., Gao, X. J., Han, Z. Y., Xu, Y., and Giorgi, F. (2021). Bias correction of temperature and precipitation over china for rcm simulations using the qm and qdm methods. *Climate Dynamics*, 57:1425–1443.

Tumsa, B. C. (2021). Performance assessment of six bias correction methods using observed and rcm data at upper awash basin, oromia, ethiopia. *Journal of Water and Climate Change*, 13(2):664–683.

USGCRP (2023). Fifth national climate assessment. Technical report.

Virtanen, P., Gommers, R., Oliphant, T. E., Haberland, M., Reddy, T., Cournapeau, D., Burovski, E., Peterson, P., Weckesser, W., Bright, J., van der Walt, S. J., Brett, M., Wilson, J., Millman, K. J., Mayorov, N., Nelson, A. R. J., Jones, E., Kern, R., Larson, E., Carey, C. J., Polat, İ., Feng, Y., Moore, E. W., VanderPlas, J., Laxalde, D., Perktold, J., Cimrman, R., Henriksen, I., Quintero, E. A., Harris, C. R., Archibald, A. M., Ribeiro, A. H., Pedregosa, F., van Mulbregt, P., and SciPy 1.0 Contributors (2020). SciPy 1.0: Fundamental Algorithms for Scientific Computing in Python. *Nature Methods*, 17:261–272.

Wang, J. and Kotamarthi, V. R. (2014). Downscaling with a nested regional climate model in near-surface fields over the contiguous united states. *Journal of Geophysical Research: Atmospheres*, 119(14):8778–8797.

Wang, J. and Kotamarthi, V. R. (2015). High-resolution dynamically downscaled projections of precipitation in the mid and late 21st century over north america. *Earth's Future*, 3(7):268–288.

Wang, L. and Chen, W. (2014). Equiratio cumulative distribution function matching as an improvement to the equidistant approach in bias correction of precipitation. *Atmospheric Science Letters*, 15(1):1–6.

Wood, A. W. (2002). Long-range experimental hydrologic forecasting for the eastern united states. *Journal of Geophysical Research*, 107(D20).

Wood, A. W., Leung, L. R., Sridhar, V., and Lettenmaier, D. P. (2004). Hydrologic implications of dynamical and statistical approaches to downscaling climate model outputs. *Climatic Change*, 62(1):189–216.

Wu, Z. and Huang, N. E. (2009). Ensemble empirical mode decomposition: a noise-assisted data analysis method. *Advances in adaptive data analysis*, 1(01):1–41.

Xu, Z., Han, Y., Tam, C.-Y., Yang, Z.-L., and Fu, C. (2021). Bias-corrected cmip6 global dataset for dynamical downscaling of the historical and future climate (1979–2100). *Scientific Data*, 8(1):293.

Xu, Z. and Yang, Z.-L. (2015). A new dynamical downscaling approach with gcm bias corrections and spectral nudging. *Journal of Geophysical Research: Atmospheres*, 120(8):3063–3084.